Aurora A and B Overexpression and Centrosome Amplification in Early Estrogen-Induced Tumor Foci in the Syrian Hamster Kidney: Implications for Chromosomal Instability, Aneuploidy, and Neoplasia

Adrianne E. Hontz,[1] Sara Antonia Li,[1] Wilma L. Lingle,[2] Vivian Negron,[2] Amy Bruzek,[2] Jeffrey L. Salisbury,[2] and Jonathan J. Li[1]

[1]Hormonal Carcinogenesis Laboratory, Department of Pharmacology, Toxicology, and Therapeutics, University of Kansas Medical Center, Kansas City, Kansas and [2]The Tumor Biology Program, Division of Experimental Pathology, Mayo Clinic and Foundation, Rochester, Minnesota

Abstract

Estrogen-induced Syrian hamster tumors in the kidney represent a useful model to gain insight into the role of estrogens in oncogenic processes. We provided evidence that early tumor foci in the kidney arise from interstitial ectopic uterine-like germinal stem cells, and that early tumor foci and well-established tumors are highly aneuploid (92–94%). The molecular mechanisms whereby estrogens mediate this process are unclear. Here, we report that estrogen treatment induced significant increases in Aurora A protein expression (8.7-fold), activity (2.6-fold), mRNA (6.0-fold), and Aurora B protein expression (4.6-fold) in tumors, compared with age-matched cholesterol-treated kidneys. Immunohistochemistry revealed that this increase in Aurora A and B protein expression was essentially confined to cells within early and large tumor foci at 3.5 and 6 months of estrogen treatment, respectively. Upon estrogen withdrawal or coadministration of tamoxifen for 10 days, a 78% to 79% and 81% to 64% reduction in Aurora A and B expression, respectively, were observed in primary tumors compared with tumors continuously exposed to estrogens. These data indicate that overexpressed Aurora A and B in these tumors are under estrogen control via estrogen receptor α. Aurora A coenriched with the centrosome fraction isolated from tumors in the kidney. Centrosome amplification (number and area/cell) was detected in early tumor foci and large tumors but not in adjacent uninvolved or age-matched control kidneys. Taken together, these data indicate that persistent overexpression of Aurora A and B is under estrogen control, and is coincident with centrosome amplification, chromosomal instability, and aneuploidy, and represent an important mechanism driving tumorigenesis. [Cancer Res 2007;67(7):2957–63]

Introduction

Estrogen-induced Syrian hamster tumors of the kidney have been intensively studied in an effort to gain a better understanding of the role of estrogenic hormones in oncogenic processes (1–4). Importantly, 100% tumor incidence is achieved in animals with a relatively modest elevation in serum estradiol-17β (E_2) concentrations ($\sim 2.3 \pm 0.4$ nmol/L/mL) and very low E_2 concentrations in renal tissue (4.6 pg/mg protein; ref. 5). These E_2 levels are comparable with those reported in human breast tissue in cycling women ($\sim 5.2–5.8$ pg/mg protein; refs. 6, 7).

These E_2-elicited tumors arise in the kidney from ectopic uterine-like germinal stem cells found in the interstitium and primarily located in the corticomedullary region, the earliest region in kidney development (8–10). Moreover, complimentary cytogenetic techniques have clearly shown that both E_2-induced early tumorous lesions and primary tumors of the kidney are highly aneuploid (92–94%; refs. 8, 11). They occur coincident with, and may be downstream consequences of c-*myc*/MYC overexpression, c-*myc* amplification, and deregulation of the cell cycle; i.e., overexpressed cyclins D1, E, cdk2 and cdk4, and MDM2 driven by estrogen receptor α (ERα; refs. 12, 13). However, it is presently unclear how E_2-induced deregulation of c-*myc* and cell cycle entities result in large-scale genomic instability and tumorigenesis.

Recently, it has been proposed that the elevated expression of mitotic kinases, especially Aurora A and B, are crucial events in the cascade leading to centrosome amplification, chromosomal instability, and aneuploidy, thus, driving oncogenesis (14, 15). The Aurora family of serine/threonine kinases is essential for the orderly progression of mitosis (16, 17). Aurora A, the most intensively studied mitotic kinase, localizes to centrosomes, has a critical role in regulating centrosome duplication, maturation, and separation, spindle assembly and stability, as well as chromosome condensation, segregation, and cytokinesis (14–17). Importantly, Aurora A overexpression has been shown to elicit neoplastic transformation in mammalian cells, both *in vivo* and *in vitro* (18–20), thus behaving as a bona fide oncogene. It is noteworthy that Aurora kinase (A/B) expression is nominal in resting cells and transiently detectable in normal proliferating cells (21, 22). The levels of Aurora B mRNA and protein expression, like those of Aurora A, peak at G_2-M phase, and their maximum kinase activity is attained at the transition from metaphase to the completion of mitosis (14, 16). Present evidence indicates that Aurora B, considered a passenger protein, targets the centromere at metaphase to phosphorylate histone H3, regulates proper chromosome segregation, and translocates the inner centromere protein (INCENP) and possibly survivin to the spindle mid-zone required for the regulation of cytokinesis. Thus, Aurora B is a key regulator of accurate chromosome segregation via the control of microtubule-kinetochore attachment and cytokinesis (16, 23–25).

In the current study, we show for the first time a concerted and sustained overexpression of both Aurora A and B and coincident centrosome amplification in solely E_2-induced early tumorous foci

Requests for reprints: Jonathan J. Li, Department of Pharmacology, Mail Stop 1018, University of Kansas Medical Center, 3901 Rainbow Boulevard, Kansas City, KS 66160. Phone: 913-588-4758; Fax: 913-588-4740; E-mail: jli1@kumc.edu.

doi:10.1158/0008-5472.CAN-06-3296

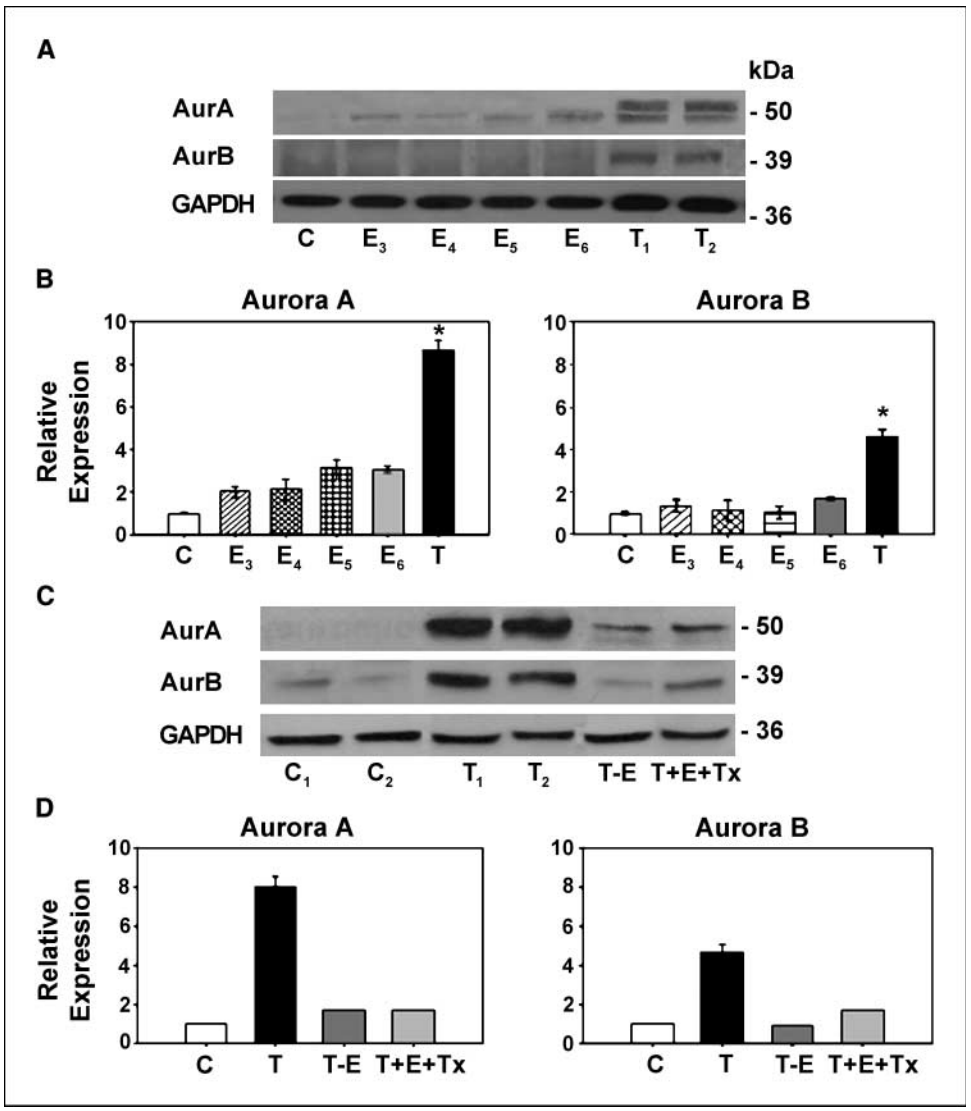

Figure 1. *A,* Western blot analysis of Aurora A and B from Syrian hamster kidneys treated with cholesterol (*C*), E_2 for 3 (E_3), 4 (E_4), 5 (E_5), or 6 (E_6) months, and E_2-induced kidney tumors (T_1 and T_2; $n = 6$). The expression of Aurora A was generally consistent in samples from cholesterol-treated control and early E_2-treated kidney samples. After 6 months of E_2 treatment, there was a slight increase in Aurora A expression followed by a marked increase in E_2-induced tumors. The tumor samples displayed the presence of a doublet, which may represent the native and phosphorylated forms of Aurora A. Aurora B expression was detected only in E_2-induced tumor samples. Glyceraldehyde-3-phosphate dehydrogenase was used as a loading control. *B,* relative expression of Aurora A and B. E_2-induced tumor samples showed a significant increase in Aurora A and B protein expression as compared with control cholesterol-treated kidney samples ($n = 6$). *C,* Western blot analysis of the modulation of Aurora kinase expression by estrogens. The expressions of Aurora A and B were determined ($n = 3$/group) in 6-month age-matched kidney samples from control cholesterol-treated animals (C_1 and C_2) and in tumors from animals continuously treated with E_2 (T_1 and T_2), 10-day withdrawal of E_2 ($T-E$), and 10-day concomitant treatment with tamoxifen citrate ($T + E + Tx$). A significant decline in Aurora A and B expression was observed after a 10-day withdrawal period of E_2 and after concomitant treatment with tamoxifen citrate. *D,* Aurora A and B relative expression. *Columns,* mean; *bars,* SE. Statistical significance was determined by one-way ANOVA with a Tukey post hoc test; *, $P < 0.001$ versus control.

and in large, well-established tumors in the hamster kidney. These findings further support the concept that E_2-mediated oncogenesis occurs by a common pathway via sustained Aurora kinase overexpression, which in turn, generates amplified centrosomes, chromosomal instability, aneuploidy, and tumor formation.

Materials and Methods

Animals. Adult castrated male Syrian golden hamsters (LAK/LVG), outbred strain, weighing 90 to 100 g were purchased from Harlan Sprague-Dawley, Inc. (Indianapolis, IN). Hamsters were housed in facilities certified by the American Association for the Accreditation of Laboratory Animal Care. They were acclimated for at least 1 week prior to use, maintained on a 12-h light/12-h dark cycle, fed certified rodent chow (Ralston-Purina 5002), and tap water *ad libitum*. The animal studies were carried out in adherence to the guidelines established in the "Guide for the Care and Use of Laboratory Animals," U.S. Department of Health and Human Resources (NIH 1985). Hamsters in the treatment groups were implanted s.c. with 20 mg E_2 pellets as described previously (26). Age-matched control animals were implanted with 20 mg pellets of cholesterol. To maintain constant levels, new pellets were implanted every 3 months. Their mean daily absorption was 96 ± 4 μg/d. The pellets were prepared by Hormone Pellet Press (Shawnee Mission, KS). Over a 6-month period of E_2 treatment, the average E_2 concentration in serum was 2.28 ± 0.43 ng/mL, and 4.57 ± 1.04 pg/mg protein in the kidney (5). Groups of five to eight castrated cholesterol-treated and E_2-treated hamsters were used for 3 to 8 months in most of the studies described. For the withdrawal studies, hamsters bearing tumors treated for 6 months with two 20-mg pellets of E_2, were divided into four groups ($n = 3$): animals in group 1 were maintained on E_2 pellets; group 2 had their two pellets removed; and those in group 3 had the initial E_2 pellet removed, whereas the second one remained and were additionally implanted with two pellets of 20 mg tamoxifen citrate; group 4 included age-matched cholesterol-treated controls. All animals were killed 10 days after the removal of the E_2 pellets and tamoxifen citrate treatment. Tumors were individually harvested from groups 1 to 3 (and kidneys from group 4) for subsequent analysis of Aurora A expression and centrosome amplification.

Western blot. Kidneys and tumors were homogenized in lysis buffer containing 50 mmol/L of Tris-HCl (pH 7.4), 0.2 mol/L of NaCl, 2 mmol/L of EDTA, 0.5% NP40, 50 mmol/L of NaF, 0.5 mmol/L of Na_3VO_4, 20 mmol/L of Na-pyrophosphate, 1 mmol/L of phenylmethylsulfonyl fluoride, 10 μg/mL of aprotinin, 10 μg/mL of leupeptin, and 1 mmol/L of DTT. The supernatant fractions were collected and their protein content determined with bicinchoninic acid reagents (Pierce, Rockford, IL). Proteins were separated by gel electrophoresis on PAGEr Gold Precast Gels (Cambrex Bio Science Rockland, Inc., Rockland, ME) and transferred to a nitrocellulose membrane. Primary antibodies against Aurora A BL656 (1:1,000; Bethyl Labs, Montgomery, TX), Aurora B ab2254 (1:1,000; Abcam, Cambridge, MA),

Centrin MCI (1:25,000; Salisbury, JL, Mayo Clinic, Rochester, MN), and γ-tubulin MMR58 (1:10,000; Salisbury, JL), were incubated overnight at 4°C. Appropriate secondary antibodies were incubated for 2 h and protein expression was visualized with enhanced chemiluminescence (Amersham Biosciences, Piscataway, NJ). Densitometry was done using Alpha Imager 2000 (Alpha Innotech, San Leandro, CA).

***In vitro* protein kinase assay.** Proteins were extracted as described for Western blotting. Aliquots, 200 μg of total protein extracts, were incubated for 2 h at room temperature with 1 μg of Aurora A BL469 (Bethyl Labs) followed by a 2-h incubation with 30 μL of A/G agarose slurry. Normal IgG was used as a negative control. Immunoprecipitated complexes were washed several times with PBS and immediately used for kinase assays (Upstate, Inc., Charlottesville, VA) following the manufacturer's standard protocol with modifications. Immunoprecipitates were incubated for 30 min at 30°C with 5× reaction buffer [40 mmol/L MOPS (pH 7.0), 1 mmol/L EDTA], 10 μCi/μL of [^{32}P]γATP (Amersham Biosciences) diluted in Upstate Mg/ATP cocktail. Reactions were spotted onto P81 paper, subjected to a series of washes in 0.75% phosphoric acid and acetone, and counts per minute measured using a scintillation counter (Beckman Coulter, Fullerton, CA).

Reverse transcriptase PCR and real-time PCR. All reagents for reverse transcriptase and real-time PCR were purchased from Invitrogen Corp., Carlsbad, CA. Total RNA was extracted using the protocol supplied by Life Technologies (Gaithersburg, MD) for Trizol Reagent. Aliquots, ~100 mg of hamster kidney tissue and E_2-induced primary tumors were immediately frozen in liquid nitrogen and pulverized while still frozen. The pulverized tissue was then placed into 3 mL of Trizol and homogenized using a Polytron. All samples were centrifuged at 12,000 × *g* for 10 min at 4°C. The supernatant was then transferred to a fresh tube and incubated at room temperature for 5 min before adding 0.2 mL of chloroform/1 mL of Trizol. The tubes were capped, shaken vigorously, and incubated for 3 min at room temperature. The tubes were centrifuged at 12,000 × *g* for 15 min at 4°C. Total RNA was then precipitated with 0.5 mL of isopropanol/1 mL of Trizol. The tubes were incubated at −80°C for 30 min and then centrifuged at 12,000 × *g* for 10 min at 4°C. The RNA pellet was washed in 1 mL of 75% ethanol/diethyl pyrocarbonate and centrifuged at 7,500 × *g* for 5 min at 4°C. After briefly drying, the pellet was resuspended in 100 μL of diethyl pyrocarbonate water and stored at −80°C. RNA integrity was evaluated by agarose gel electrophoresis and the concentration of the RNA was determined by spectrometry.

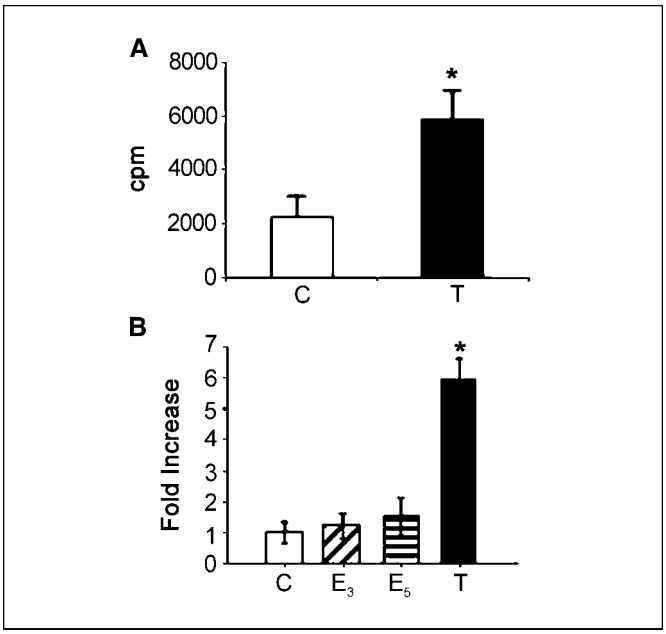

Figure 2. *A* and *B,* Aurora A kinase activity and real-time PCR for Aurora A. *A,* a significant increase in Aurora A kinase activity was observed in E_2-induced hamster kidney tumor samples (*T*) when compared with cholesterol-treated control (*C*) hamster kidneys ($n = 6$); *t* test; *, $P < 0.05$. *B,* Aurora A mRNA levels were analyzed by real-time PCR. A significant 6-fold increase was detected in E_2-induced tumor samples compared with cholesterol-treated control samples ($n = 6$). *Columns,* mean; *bars,* SE. Statistical significance was determined by one-way ANOVA with a Tukey post hoc test; **, $P < 0.001$ versus control, E_2-treated for 3 (E_3) and 5 months (E_5), and tumor samples.

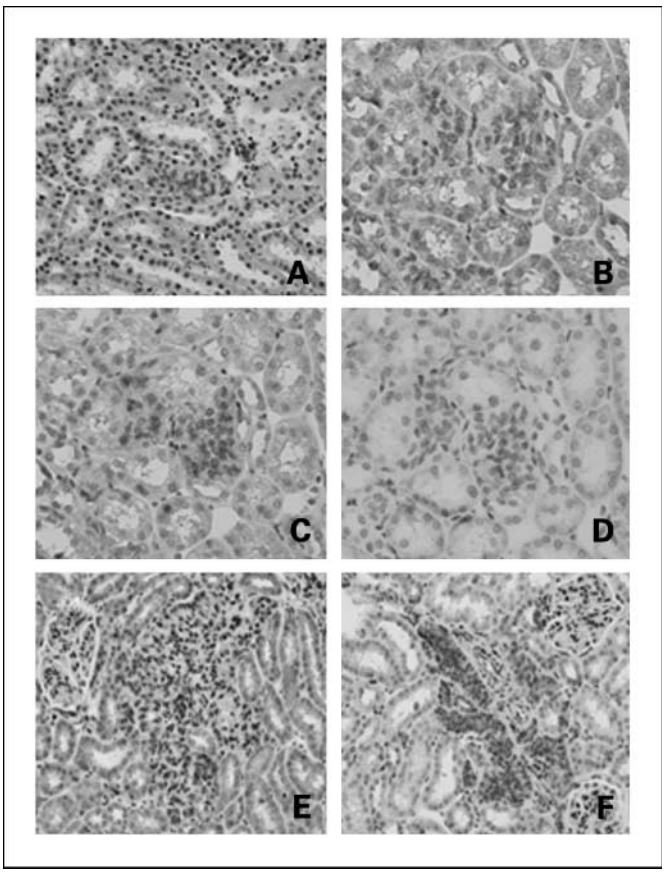

Figure 3. *A* to *F,* representative kidney serial sections from 3.5- and 6-month E_2-treated hamster kidneys sequentially stained for H&E and Aurora A and B (*A–D*). *A,* H&E representative kidney section from a 3.5-month E_2-treated hamster kidney showing a small tumor focus. *B* and *C,* Aurora A and B. The cells present in the tumor foci were Aurora A (*B*) and Aurora B (*C*) positive. *D,* kidney serial section without primary antibodies. *E* and *F,* representative 6-month E_2-treated hamster kidney sections stained for Aurora A (*E*) and Aurora B (*F*). Aurora A and Aurora B positive stained cells were confined to the tumor foci (magnification, ×40).

Reverse transcription was done using 5 μg of total RNA/5 μL. The RNA was combined with 250 ng of random primers, 10 mmol/L of deoxynucleotide triphosphate mix, and sterile distilled water. This mixture was heated at 65°C for 5 min and quick-chilled on ice. 5× first strand buffer, 0.1 mol/L of DTT, and Moloney murine leukemia virus reverse transcriptase was added to each sample and the reverse transcription reaction was done using an iCycler thermocycler (Bio-Rad Laboratories, Hercules, CA). The thermocycling protocol consisted of 1 h incubation at 37°C followed by 10 min incubation at 96°C. The samples were stored at 4°C until used for PCR analysis.

The cDNA synthesized during the reverse transcription reaction was used to perform the real-time PCR reaction. cDNA was amplified using the Platinum SYBR Green qPCR SuperMix UDG and gene-specific primers for β-actin (FWD 5-CAGCCGAGAGGGAAATTGTG-3′; REV 5-TCGTTGCCAATGGTGATGAC-3′; 101 bp amplicon) and Aurora A (FWD 5-TGGGTGTGTGCCTCGAAA; REV 5-GATTGAAGGCCGGATGCA; 102 bp amplicon) in a 7300 Real-time PCR System (Applied Biosystems, Foster City, CA). *Myc* gene amplification was used as a positive control (FWD 5-TGATGTCGTGTCTGTGGAAAAGA; REV 5-GTTTGCTGTGGCCTCCTGAT; 83 bp amplicon). The

baseline was set automatically, as was the threshold Ct value measured during the exponential phase of the amplification. The thermocycling protocol consisted of 2 min incubation at 50°C followed by 10 min incubation at 95°C. Then, the samples underwent 40 cycles at 95°C for 45 s, 60°C for 45 s, and 72°C for 45 s. The specificity of the amplicon was verified by running a dissociation step.

Immunohistochemical analysis. Kidneys were excised, trimmed, and fixed in 5% paraformaldehyde, followed by a rapid paraffin-embedding process. Tissue sections (6 μm) were prepared and dewaxed. Antigens were retrieved (Dako Target Retrieval Solution; Dako, Carpinteria, CA) by heating in a water bath set at 97°C for 20 min or a digital decloaking chamber (Biocare Medical, Concord, CA) and treated with 3% H_2O_2 for 15 min to block endogenous peroxidases. After blocking with 6% of the appropriate serum in 1% bovine serum albumin, the primary antibodies, ERα clone 1D5 (Dako), progesterone receptor (PR) C-19 (Santa Cruz Biotechnology, Santa Cruz, CA), Aurora A BL656 (Bethyl Labs), and Aurora B ab2254 (Abcam), diluted 1:50 (1:1,000 for Aurora A), were applied to the sections overnight at 4°C. Appropriate secondary antibodies were incubated for 1 h at 25°C followed by 1 h with Vector Laboratories Elite ABC (Burlingame, CA). As negative controls, similar tissue sections were incubated replacing the primary antibodies with the appropriate normal serum. The slides were counterstained with hematoxylin, dehydrated in alcohol, and mounted in Permount medium (1:1 permount/xylene) before being examined under the microscope.

Enrichment of amplified tumor centrosomes. The isolation of amplified E_2-induced tumor centrosomes was done according to Moudjou and Bornens (27) with minor modifications. Primary tumors (8–10 g) from the kidney were minced and brought to 50 mL in culture medium containing 10 μL cytochalasin, 10 μL nocodazole, and 50 μL protease inhibitor cocktail, all obtained from Sigma (St. Louis, MO). The minced tumor was incubated for 30 min at 4°C, washed and then resuspended in 0.1× TBS/8% sucrose containing 2 μL of cytochalasin, 2 μL of nocodazole, and 10 μL of protease inhibitor cocktail and pressed through a stainless steel sieve and filtered through a 105-μm nylon mesh monofilament cloth (Small Parts, Inc., Miami Lakes, FL). The resulting cell suspension was lysed in a buffer containing 1 mmol/L of Tris-HCl (pH 8.0), 0.1% 2-mercaptoethanol, 0.5% Triton X-100, and 1× protease inhibitors, homogenized in a glass dounce, and centrifuged at 2,500 × *g* for 10 min. The lysate was placed in a 50 mL tube, underlaid with 60% sucrose, and centrifuged at 10,000 × *g* for 30 min. The upper 25 mL fraction was carefully aspirated off, and the remaining sample was vortexed, overlaid onto a vegetable-dyed sucrose gradient (70%, 50%, and 40% sucrose), and centrifuged at 40,000 × *g* for 1 h. The gradient was fractionated into 25 0.5-mL portions [Fraction Collector and Econo Pump (Bio-Rad Laboratories) Fractionation System (Brandel, Gaithersburg, MD)]. The fraction volumes were brought to 1.5 mL with gradient buffer [10 mmol/L PIPES (pH 7.2), 0.1% Triton X-100 and 0.1% 2-mercaptoethanol], vortexed, and centrifuged at 50,000 × *g* for 1 h. The supernatant was discarded and the pelleted fractions were stored at −80°C for further analysis.

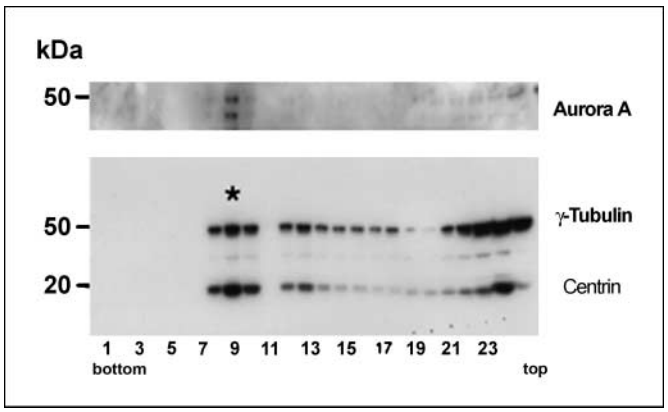

Figure 4. Centrosome isolation fractions from a combined sample of E_2-induced kidney tumors depicting the presence of Aurora A, γ-tubulin, and centrin. Note that the Aurora A expression peak is located in fraction 9, where a major peak for γ-tubulin and centrin expression is also present.

Centrosome amplification: size and number. Centrosome size and number were analyzed by confocal microscopy of paraffin sections immunolabeled with a monoclonal antibody against the centrosomal protein γ-tubulin (28). Kidney tissues from age-matched control and E_2-treated hamsters for 3, 4, and 8 months were analyzed (n = 3/group). For centrosome evaluation in tumor lesions, tumor foci were first identified in serial sections stained with H&E and PR (C19) from Santa Cruz Biotechnology. Once the foci were identified, subsequent serial sections were immunolabeled with γ-tubulin and Hoechst 33342, to label the centrosomes and the nuclei, respectively (29). Confocal image stacks of seven 5-μm/L-thick slices were captured with a Zeiss 510 confocal microscope using a 63× oil immersion objective. Image stacks were then processed to yield a single maximum intensity projection image. The resulting image was imported into ImageJ (NIH Image) for analysis. The γ-tubulin signal was thresholded consistently for all the images collected for each tissue. The thresholded images were then binarized and the area of each γ-tubulin–labeled spot measured and counted. Cells were counted manually according to the number of nuclei present within an image. On average, 500 cells per tissue category were analyzed; 106 cells was the minimum number analyzed. The size of the epithelial cell centrosomes were normalized against centrosomes in nearby fibroblasts. This normalization process is based on the assumption that the size of fibroblast centrosomes is consistent between the individual animals; therefore, it allows valid comparisons of centrosome size among different tissues in separate animals immunolabeled at various times, and among images captured in separate microscopy sessions. Centrosome size per cell was calculated as the combined region of all γ-tubulin–labeled areas in the image divided by the total number of cells present. Centrosomes in normal tissues are an order of magnitude smaller than nuclei; therefore, this calculation returns a value of >1 because sections through cells pass through the centrosomes less frequently than sections pass through the cell nucleus. In the average cell, the centrosome will appear in only 1/4 of the sections, whereas the nucleus, on average, will appear in essentially all sections.

Statistical analyses. One-way ANOVA with Dunn or Tukey post hoc tests were used for statistical evaluation of the data presented, with the exception of the Aurora A kinase activity and the centrosome size and number that were analyzed using t test. Values were expressed as the mean ± SE. Statistical significance was assumed when $P < 0.05$ were obtained.

Results

Western blot analysis of Aurora A and B in whole kidneys and tumors during E_2-induced oncogenesis. Protein expression of Aurora A and B kinase was determined in lysates of whole hamster kidney samples after 3, 4, 5, and 6 months, and primary tumors after 6 months of E_2 treatment (Fig. 1*A*). Although modest increases in Aurora A protein were seen in early E_2 treatment periods, a significant 8.7-fold increase was detected in primary tumors (Fig. 1*B*) when compared with control cholesterol-treated kidneys. A slower migrating Aurora A band, presumably the phosphorylated form of Aurora A, was observed only in E_2-induced tumors of the kidney. No detectable changes in Aurora B protein expression (Fig. 1*A*) were seen after 3 to 5 months of E_2 treatment. A slight increase in Aurora B expression was detected in 6-month E_2-treated kidneys. However, a significant 4.6-fold increase in Aurora B expression was seen in primary E_2-induced tumors of the kidney compared with age-matched cholesterol-treated control kidneys (Fig. 1*B*).

Modulation of Aurora kinase expression in E_2-induced tumors by either estrogen withdrawal or concomitant tamoxifen citrate treatment. Tumor samples from groups of 6-month tumor-bearing animals that were continuously E_2-treated

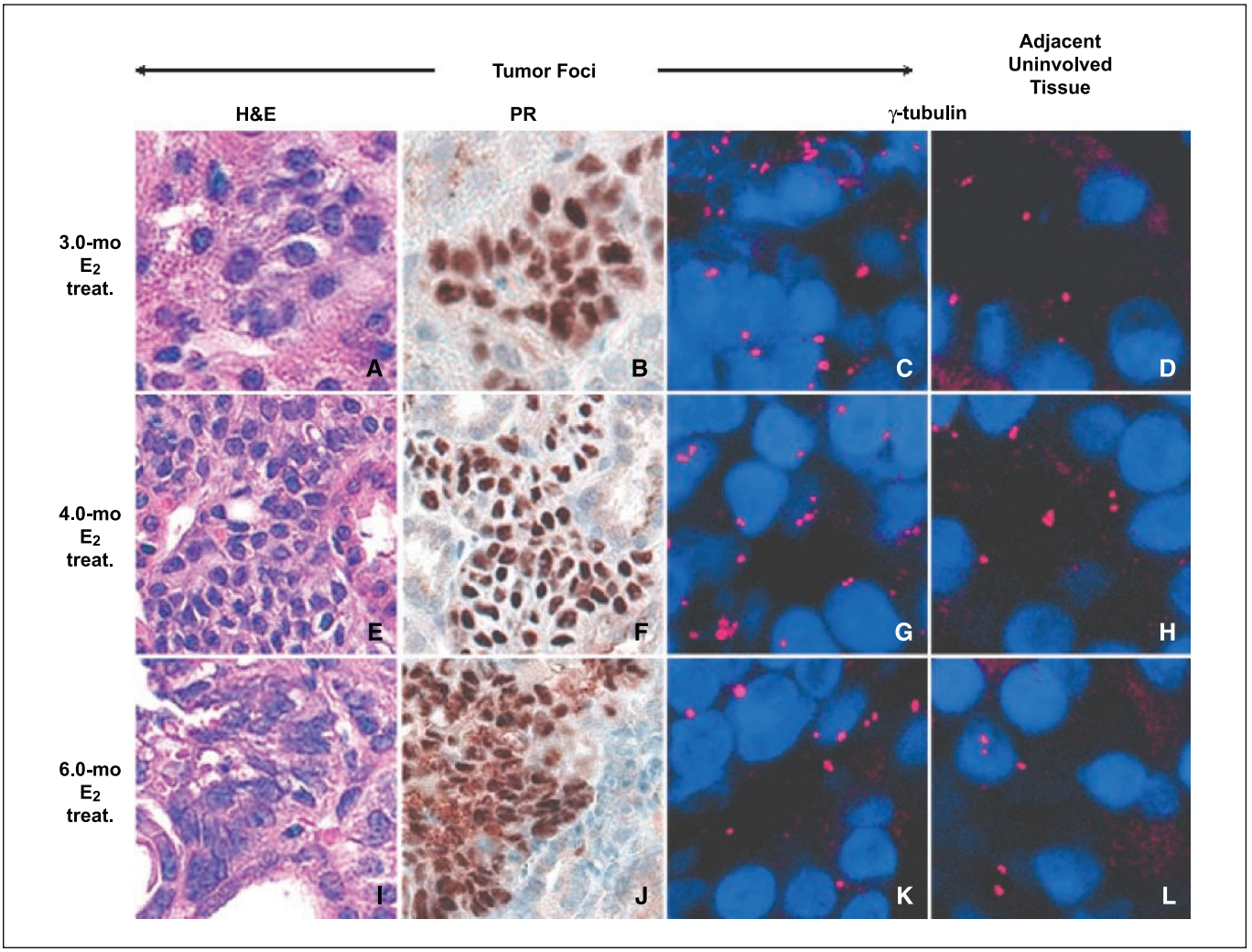

Figure 5. Centrosomes and nuclei from serial sections of early tumor foci obtained from 3-, 4- and 6-mo E_2-treated hamster kidneys (*C, G*, and *K*) and adjacent uninvolved tissue (*D, H*, and *L*) were observed by confocal microscopy labeled with an antibody against γ-tubulin (*red*) and DNA dye Hoechst 33342 (*blue*) in areas corresponding to H&E (*A, E*, and *I*) and PR (*B, F*, and *J*) stained sections. Centrosomes in adjacent uninvolved kidney cells are apical to the nucleus and often appear as a pair of adjacent spots. The size of the centrosome spots in these samples is uniform at all treatment periods. Many centrosomes in the tumor foci sections at all treatment periods (*C, G*, and *K*) are much larger and more numerous than centrosomes in adjacent uninvolved tissue (*D, H*, and *L*).

or had either their E_2 pellets withdrawn or concomitantly treated with tamoxifen citrate for 10 days were analyzed for Aurora A and B expression by Western blot. The withdrawal/treatment period was selected because we have previously shown that 72 h are required to completely clear estrogens from the serum of treated animals (5). Compared with age-matched control cholesterol-treated kidneys, an 8.0-fold increase in Aurora A expression was detected in all tumors receiving sustained E_2 treatment (Fig. 1*D*). Upon 10-day estrogen withdrawal, Aurora A expression was significantly reduced by 78% compared with tumors continuously treated with E_2. Similarly, coadministration with tamoxifen citrate also resulted in a significant 79% decline in Aurora A expression in these tumors. Correspondingly, E_2-elicited Aurora B overexpression also markedly declined when E_2 was withdrawn (81%) or tamoxifen citrate (64%) was coadministered. Cell proliferation, assessed by Ki-67 labeling was not significantly altered in any of the tumor groups (data not shown). Although a significant decline in the expression of Aurora A and B was observed upon E_2 withdrawal and E_2 + tamoxifen citrate treatment, a corresponding reduction in amplified centrosomes was not observed in any of these treatment groups.

Aurora A activity and mRNA levels in E_2-induced tumors. Additionally, the increased overexpression of Aurora A led to a concomitant 2.6-fold increase in its activity as detected using a synthetic construct kemptide as a substrate (Fig. 2*A*). Additionally, Aurora A mRNA also showed a significant 6.0-fold increase in primary tumors in the kidney compared with age-matched cholesterol-treated control kidneys (Fig. 2*B*).

Overexpressed Aurora A and B in early tumorous foci. In order to assess the precise cellular location of Aurora A and B expression after various E_2-treatment intervals, serial kidney sections containing early tumorous foci (Fig. 3*A*) were examined by H&E staining and immunohistochemistry. Serial sections of 3.5-month E_2-treated whole kidneys show that the expression of both Aurora A (Fig. 3*B*) and B (Fig. 3*C*) was confined essentially to cells present in early tumorous foci. No positive stained cells were detected in similar tumor foci sections in the absence of either primary antibodies (Fig. 3*D*). Positive stained Aurora A (Fig. 3*E*) and B (Fig. 3*F*) cells were also present in well-established large tumor foci derived from 6-month E_2-treated hamsters, but not in adjacent uninvolved epithelial kidney cells.

Localization of Aurora A and centrosome proteins to isolated amplified tumor centrosomes. Preparations of enriched amplified centrosomes were obtained from tumors induced after 6 to 8 months of E_2 treatment employing a discontinuous sucrose gradient fractionated into 25 aliquots (Fig. 4). Western blot analysis established that fractions 8 to 10 expressed high levels of γ-tubulin and centrin. Both centrosome proteins consistently exhibited the highest level of expression in fraction 9, whereas their expression in other fractions was variable and in reduced amounts. Notably, Aurora A expression was expressed exclusively in fraction 9, indicating that this mitotic kinase was associated solely with the amplified tumor centrosome fraction. On the other hand, Aurora B expression was distributed at least throughout fractions 6 to 10 (data not shown), as expected of a passenger protein kinase.

Centrosome amplification in early estrogen-induced tumorous foci. Small early E_2-induced tumorous foci were first detected in H&E-stained renal serial sections from hamsters treated with E_2 for 3 (Fig. 5*A*) and 4 months (Fig. 5*E*). These cell clusters of incipient tumor foci were characterized by their large pale-staining nuclei (Fig. 5*A* and *E*), PR-positive staining (Fig. 5*B* and *F*), and were not evident in age-matched cholesterol-treated kidneys. E_2-induced tumor foci, at all time periods examined (Fig. 5*C, G*, and *K*), showed a markedly elevated number of centrosomes, which were unevenly distributed in the cytoplasm compared with cholesterol-treated, age-matched, and adjacent uninvolved kidney cells (Fig. 5*D, H*, and *L*). In adjacent uninvolved kidney tissue sections from 3-, 4- and 8-month E_2-treated hamsters (Fig. 5*D, H, L*), the pattern of immunofluorescence staining of the centrosomal protein γ-tubulin was confined to the pair of centrioles apical to the nucleus. Similarly, cholesterol-treated age-matched kidney samples showed comparable levels and location of γ-tubulin immunostaining (data not shown). When 3-month E_2-induced tumorous foci were compared with age-matched untreated control kidneys, a significant 1.8-fold increase in centrosome number was observed (Fig. 6). A further significant increase in centrosome number (2.8-fold) was detected after 4 months of E_2 treatment. Well-established tumor foci also exhibited a 1.8-fold increase in centrosome number per cell. When total centrosome area per cell was determined, 2.6-, 5.4-, and 2.5-fold increases were found in 3- and 4-month early tumorous foci, and in large tumor foci after 8 months of E_2-treatment, respectively (Fig. 6). An increase in the number and total volume of centrosomes was indicative of centrosome amplification.

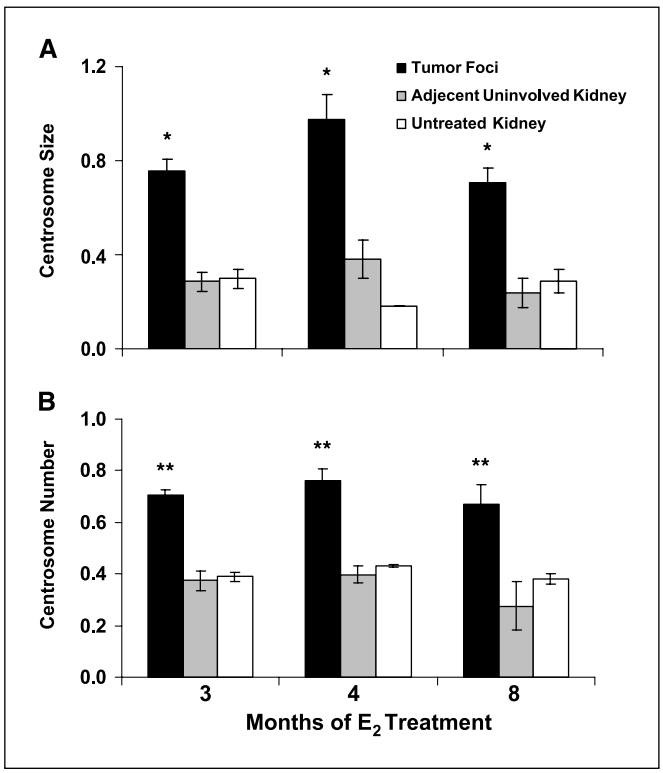

Figure 6. Centrosome size (*A*) and centrosome number (*B*) in E_2-induced early tumor foci and well-established tumors in the hamster kidney. A statistically significant increase in size and number is depicted in tumor foci from 3-, 4-, and 6-mo E_2-treated hamster kidneys compared with adjacent uninvolved and age-matched control kidney samples. *Columns,* mean from a minimum of three independent experiments; *bars,* SE; *, $P < 0.01$ for size; and **, $P < 0.02$ for number.

Discussion

Tumors arising from interstitial uterine-like germinal stem cells in the kidney are driven by estrogen interacting with ERα, and the neoplastic progression occurs in the absence of any discernible histopathologic stages (8). This E-ERα–mediated process is completely prevented by concomitant administration of either tamoxifen citrate, progesterone, or androgen competing with ERα or respective hormone binding to their specific receptors (26, 30, 31). These findings strongly indicate that tumorigenesis is mediated by an ERα-mediated process consistent with a uterine-like tissue behavior because progesterone opposes the action of estrogen in the endometrium.

The detection of high aneuploid frequencies, employing cytogenetic methodologies, nuclear image cytometry, G-banding karyotyping, comparative genomic hybridization, and fluorescence *in situ* hybridization in early tumorous lesions and in large, well-established tumors (8, 11, 13) have clearly established that chromosomal instability and aneuploidy are early events in solely E_2-induced tumors. Moreover, non-random or consistent whole chromosome gains and losses have been detected in primary tumors with a frequency of 50% to 88%, depending on the specific chromosome of all tumors examined (11). Interestingly, similar high aneuploid frequencies have been detected in E_2-induced ductal carcinoma *in situ* (DCIS) and primary breast tumors in female ACI rats, and in E_2 plus androgen-induced primary tumors in male Noble rats (32). Taken together, these findings indicate that these molecular alterations represent a common early pathway in E_2-driven oncogenic processes.

Persistent overexpression of mitotic kinases, notably Aurora A and B, has been associated with centrosome amplification, which in turn, is believed to elicit chromosomal instability and aneuploidy; key molecular changes leading to tumor formation (14–17). Nevertheless, no definitive evidence has yet shown that these events are in fact causally related. Persistent Aurora A and B overexpression in concert with centrosome amplification in early tumorous foci and in primary tumors elicited by E_2, however, is consistent with previous findings that these molecular events invariably occur together (21, 33). The early detection of Aurora A and B overexpression and centrosome amplification in 3-month tumorous foci, as reported herein, provides additional evidence that these mitotic kinases may be involved in the incipient events leading to tumor development. The discovery that Aurora A and B are persistently overexpressed in early tumorous foci in the kidney

and Aurora A in dysplasias and DCIS in female ACI rats (34), both induced by E_2, suggest that these kinases are under direct or indirect estrogen control. This notion is now supported by our finding that upon estrogen withdrawal or the coadministration of tamoxifen citrate in the presence of E_2, a marked decline in Aurora A expression was found in tumors residing in the kidney compared with corresponding tumors maintained only on E_2.

Not unexpectedly, the relative brief period of E_2 withdrawal, or E_2 + tamoxifen citrate treatment, did not result in a decrease in centrosome amplification in tumors in the kidney, even though Aurora A expression declined significantly. Centrosomes are complex structures, and the γ-tubulin and centrin present in centrosomes are relatively stable proteins. Therefore, the tumor cells likely require many cell cycles in order to deplete these proteins from the centrosome structure. Moreover, when E_2 is withdrawn or blocked, the rate of cell proliferation will eventually decrease, reducing the opportunity for changes in the contribution of these centrosome proteins to centrosome size and number.

Because estrogens are the major causative agent in human sporadic breast cancer, it is not surprising that our findings in two E_2-induced tumor rodent models replicate the high frequencies of Aurora A overexpression (~94%) and amplified centrosomes (~80%) reported in both human premalignant DCIS lesions and primary invasive ductal breast cancer (22, 28, 35). The precise relationship between the sustained overexpression of Aurora A and B and the generation of amplified centrosomes leading to multipolar spindle formation and unequal segregation of chromosomes both in E_2-induced early tumorous focal lesions in male Syrian hamster kidneys and in dysplasias/DCIS in female ACI rats remains to be resolved. Combined Aurora A and B phosphorylate more than 20 centrosomal and mitotic protein substrates (21), and the phosphorylation of individual or cassettes of their substrates might affect the deregulation of the centrosome cycle, particularly centrosome duplication.

In summary, we have shown that Aurora A overexpression and activity and Aurora B overexpression are linked to centrosome amplification, leading to chromosome instability, aneuploidy, and tumor development. These critical events occur during incipient stages of E_2-induced oncogenesis and indicate a possible common mechanism whereby estrogens elicit tumor development in target tissues.

Acknowledgments

Received 9/7/2006; revised 1/19/2007; accepted 1/25/2007.

Grant support: National Cancer Institute grants RO1 CA102849 (J.J. Li), DAMD 17-01-1-0753, The Breast Cancer Research Foundation (W.L. Lingle), and RO1 CA072836 (J.L. Salisbury).

The costs of publication of this article were defrayed in part by the payment of page charges. This article must therefore be hereby marked *advertisement* in accordance with 18 U.S.C. Section 1734 solely to indicate this fact.

References

1. Toubeau G, Nonclercq D, Laurent G, et al. Immunohistochemical analysis of diethylstilbestrol-induced renal tumors in adult male Syrian hamsters: evidence for relationship to peripheral nerve sheath tumors. Histochem Cell Biol 2001;115:429–38.
2. Cortes-Vizcaino V, Peydro-Olaya A, Llombart-Bosch A. Morphological and immunohistochemical support for the interstitial cell origin of oestrogen-induced kidney tumours in the Syrian golden hamster. Carcinogenesis 1994;15:2155–62.
3. Hacker HJ, Vollmer G, Chiquet-Ehrismann R, Bannasch P, Liehr JG. Changes in the cellular phenotype and extracellular matrix during progression of estrogen-induced mesenchymal kidney tumors in Syrian hamsters. Virchows Arch B Cell Pathol Incl Mol Pathol 1991; 60:213–23.
4. Li JJ, Weroha SJ, Cansler M, Li SA. Estrogen-receptor-mediated genomic instability in Syrian hamster kidney: A critical event in hormonal carcinogenesis. In: Li JJ, Li SA, Daling JR, editor. Hormonal carcinogenesis III: Proceedings of the Third International Symposium. New York: Springer; 2001. p. 149–57.
5. Li SA, Xue Y, Xie Q, Li CI, Li JJ. Serum and tissue levels of estradiol during estrogen-induced renal tumorigenesis in the Syrian hamster. J Steroid Biochem Mol Biol 1994;48:283–6.
6. Thijssen JH, van Landeghem AA, Poortman J. Uptake and concentration of steroid hormones in mammary tissues. Ann N Y Acad Sci 1986;464:106–16.
7. Bonney RC, Reed MJ, Davidson K, Beranek PA, James VH. The relationship between 17β-hydroxysteroid dehydrogenase activity and oestrogen concentrations in human breast tumours and in normal breast tissue. Clin Endocrinol (Oxf) 1983;19:727–39.
8. Li JJ, Weroha SJ, Davis MF, Tawfik O, Hou X, Li SA. ER and PR in renomedullary interstitial cells during Syrian hamster estrogen-induced tumorigenesis: evidence for receptor-mediated oncogenesis. Endocrinology 2001; 142:4006–14.
9. Gonzalez A, Oberley TD, Li JJ. Morphological and immunohistochemical studies of the estrogen-induced Syrian hamster renal tumor: probable cell of origin. Cancer Res 1989;49:1020–8.
10. Oberley TD, Gonzalez A, Lauchner LJ, Oberley LW, Li JJ. Characterization of early kidney lesions in estrogen-induced tumors in the Syrian hamster. Cancer Res 1991; 51:1922–9.
11. Papa D, Li SA, Li JJ. Comparative genomic hybridization of estrogen-induced ectopic uterine-like stem cell neoplasms in the hamster kidney: nonrandom chromosomal alterations. Mol Carcinog 2003;38:97–105.
12. Liao DZ, Hou X, Bai S, Li SA, Li JJ. Unusual deregulation of cell cycle components in early and frank estrogen-induced renal neoplasias in the Syrian hamster. Carcinogenesis 2000;21:2167–73.
13. Li JJ, Hou X, Banerjee SK, et al. Overexpression and amplification of c-myc in the Syrian hamster kidney during estrogen carcinogenesis: a probable critical role in neoplastic transformation. Cancer Res 1999;59:2340–6.
14. Katayama H, Brinkley WR, Sen S. The Aurora kinases: role in cell transformation and tumorigenesis. Cancer Metastasis Rev 2003;22:451–64.
15. Marumoto T, Zhang D, Saya H. Aurora-A—a guardian of poles. Nat Rev Cancer 2005;5:42–50.
16. Nigg EA. Mitotic kinases as regulators of cell division and its checkpoints. Nat Rev Mol Cell Biol 2001;2:21–32.
17. Goepfert TM, Brinkley BR. The centrosome-associated Aurora/Ipl-like kinase family. Curr Top Dev Biol 2000;49:331–42.
18. Bischoff JR, Anderson L, Zhu Y, et al. A homologue of Drosophila aurora kinase is oncogenic and amplified in human colorectal cancers. EMBO J 1998;17:3052–65.
19. Tatsuka M, Katayama H, Ota T, et al. Multinuclearity and increased ploidy caused by overexpression of the aurora- and Ipl1-like midbody-associated protein mitotic kinase in human cancer cells. Cancer Res 1998;58:4811–6.
20. Zhou H, Kuang J, Zhong L, et al. Tumour amplified kinase STK15/BTAK induces centrosome amplification, aneuploidy and transformation. Nat Genet 1998;20:189–93.
21. Li JJ, Li SA. Mitotic kinases: The key to duplication, segregation, and cytokinesis errors, chromosomal instability, and oncogenesis. Pharmacol Ther 2006;111:974–84.
22. Tanaka T, Kimura M, Matsunaga K, Fukada D, Mori H, Okano Y. Centrosomal kinase AIK1 is overexpressed in invasive ductal carcinoma of the breast. Cancer Res 1999;59:2041–4.
23. Vagnarelli P, Earnshaw WC. Chromosomal passengers: the four-dimensional regulation of mitotic events. Chromosoma 2004;113:211–22.
24. Sampath SC, Ohi R, Leismann O, Salic A, Pozniakovski A, Funabiki H. The chromosomal passenger complex is required for chromatin-induced microtubule stabilization and spindle assembly. Cell 2004;118: 187–202.
25. Ota T, Suto S, Katayama H, et al. Increased mitotic phosphorylation of histone H3 attributable to AIM-1/Aurora-B overexpression contributes to chromosome number instability. Cancer Res 2002;62:5168–77.
26. Li JJ, Cuthbertson TL, Li SA. Inhibition of estrogen tumorigenesis in the Syrian golden hamster kidney by antiestrogens. J Natl Cancer Inst 1980;64:795–800.
27. Moudjou M, Bornens M. Cell biology: a laboratory handbook. San Diego: Academic Press; 1994.
28. Lingle WL, Lutz WH, Ingle JN, Maihle NJ, Salisbury JL. Centrosome hypertrophy in human breast tumors: implications for genomic stability and cell polarity. Proc Natl Acad Sci U S A 1998;95:2950–5.
29. Carroll PE, Okuda M, Horn HF, et al. Centrosome hyperamplification in human cancer: chromosome instability induced by p53 mutation and/or Mdm2 overexpression. Oncogene 1999;18:1935–44.
30. Li JJ, Li SA. Estrogen-induced progesterone receptor in the Syrian hamster kidney. II. Modulation by synthetic progestins. Endocrinology 1981;108:1751–6.
31. Li JJ, Li SA. Estrogen carcinogenesis in hamster tissues: a critical review. Endocr Rev 1990;11:524–31.
32. Li JJ, Papa D, Davis MF, et al. Ploidy differences between hormone- and chemical carcinogen-induced rat mammary neoplasms: comparison to invasive human ductal breast cancer. Mol Carcinog 2002;33:56–65.
33. Brinkley BR, Goepfert TM. Supernumerary centrosomes and cancer: Boveri's hypothesis resurrected. Cell Motil Cytoskeleton 1998;41:281–8.
34. Li JJ, Weroha SJ, Lingle WL, Papa D, Salisbury JL, Li SA. Estrogen mediates Aurora-A overexpression, centrosome amplification, chromosomal instability, and breast cancer in female ACI rats. Proc Natl Acad Sci U S A 2004;101:18123–8.
35. Lingle WL, Barrett SL, Negron VC, et al. Centrosome amplification drives chromosomal instability in breast tumor development. Proc Natl Acad Sci U S A 2002;99: 1978–83.

Aurora A and B Overexpression and Centrosome Amplification in Early Estrogen-Induced Tumor Foci in the Syrian Hamster Kidney: Implications for Chromosomal Instability, Aneuploidy, and Neoplasia

Adrianne E. Hontz, Sara Antonia Li, Wilma L. Lingle, et al.

Cancer Res 2007;67:2957-2963.